ChemComm

COMMUNICATION

View Article Online
View Journal | View Issue

Cite this: *Chem. Commun.*, 2024, **60**, 6512

Received 18th March 2024,
Accepted 26th May 2024

DOI: 10.1039/d4cc01232a

rsc.li/chemcomm

Giant anisotropic thermal expansion of copper-cyanido flat layers with flexible copper nodes†

Yuudai Iwai,[a] Manabu Nakaya,[b] Yuta Tsuji,[c] Benjamin Le Ouay,[a] Masaaki Ohba *[a] and Ryo Ohtani *[a]

Flat layers are usually considered as structurally rigid motifs in two-dimensional (2D) materials. In this work, we demonstrate that a flat honeycomb-layer composed of distorted tri-coordinate copper ions bridged with cyanidos in (tetraethylammonium)$Cu_2(CN)_3$ exhibits high in-plane flexibility. This resulted in an extremely large anisotropic 2D-thermal expansion.

Two-dimensional (2D) materials have attracted attention due to their functionalities coupled with large anisotropy of the layer between the in-plane and stacking directions. The flexibility of each individual layer, coupled with the change of chemical and physical properties, is a key structural feature for exploring functionalities such as adsorption,[1,2] magnetism,[3,4] and electronic properties.[5,6] Thus, unveiling the relationship between a flexible structure and a response to stimuli for layers is of high significance not only for deepening fundamental insights on 2D-materials but also for the development of future devices utilizing thin films[7,8] and membranes.[9,10]

The motif of layer structures, such as flat and undulation, significantly influences the anisotropic structural transformation. For example, undulating layers in uniaxial[11,12] and biaxial[13–16] directions are highly flexible due to the anisotropic and isotropic structural transformations, respectively, involving layer-expansion/contraction (Fig. 1). By contrast, flat layers tend generally to be rigid and less anisotropic in their in-plane directions.[17,18] These relationships between layer-motif and flexibility have been demonstrated by various 2D-materials such as graphene,[19–21] covalent-organic frameworks[22–24] and coordination polymers (CPs)/metal–organic frameworks.[25–27]

2D-CPs are modern materials that exhibit the designability of layer structures constructed by metal ions connected with ligands *via* coordination bonds. These relatively dynamic connections provide characteristic structural flexibility, giving rise to various thermal expansion (TE) behavior. Our group has reported about composition-dependent TE of several cyanido-bridged 2D-CPs such as Mn(solv.)$[Pd(CN)_4]\cdot x$solv. (solv. = H_2O, and MeOH),[28] $[Mn(salen)]_2[M(CN)_4]\cdot xH_2O$ (M = Pt, PtI_2, and MnN),[29] and $(PPh_4)Cu_2(CN)_3$ (**PPh_4Cu**; PPh_4^+ = tetraphenylphosphonium),[30] proving the structure-flexibility relationship of flexible-undulating and rigid-flat layers. Notably, flat honeycomb layers of **PPh_4Cu** were very rigid with zero area thermal expansion involving a double distortion relaxation mechanism involving a

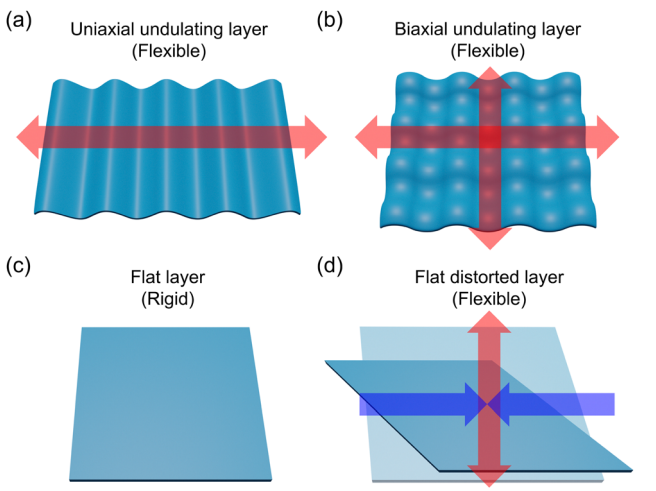

Fig. 1 Schematics displaying the relationships between layer-motifs and structural flexibility. Flexible layers with (a) uniaxial and (b) bi-axial undulation. (c) A conventional flat and rigid layer. (d) Flat but flexible distorted layer, demonstrated in this work. Arrows indicate directions of layer-deformation.

[a] *Department of Chemistry, Faculty of Science, Kyushu University, 744 Motooka, Nishi-ku, Fukuoka 819-0395, Japan. E-mail: ohba@chem.kyushu-univ.jp, ohtani@chem.kyushu-univ.jp*
[b] *Department of Chemistry, Faculty of Science, Josai University, 1-1 Keyakidai, Sakado, Saitama 350-0295, Japan*
[c] *Faculty of Engineering Sciences, Kyushu University, Kasuga, Fukuoka 816-8580, Japan*

† Electronic supplementary information (ESI) available: Experimental details including preparation and characterization of materials, crystal parameters, IR and Raman spectra, TG curve, and calculation results. CCDC 2337198–2337204. For ESI and crystallographic data in CIF or other electronic format see DOI: https://doi.org/10.1039/d4cc01232a

Table 1 CTEs of **TEACu** and **PPh_4Cu**[30] (* indicates stacking directions)

CTE (MK^{-1})	*a*	*b*	*c*	*V*
TEACu	−34.7(4)	70.9(9)	132(20)*	168.2(28)
PPh_4Cu	5.5(3)	86(3)*	−5.3(3)	86.2(14)

coupling of structural changes of the PPh_4^+ and $[Cu_2(CN)_3]^-$ counterparts (Table 1). Such strongly coupled behaviour between the honeycomb layers and sandwiched cations motivated us to explore other counter-cations to bring out the unusual flexibility of the flat layers.[31]

Herein, we report that a flat honeycomb layer of (tetraethylammonium)$[Cu_2(CN)_3]$ (**TEACu**)[32] is highly flexible, giving rise to giant anisotropic in-plane thermal expansion whose coefficients are $-34.7\ MK^{-1}$ ($M = 10^6$) and $70.9\ MK^{-1}$. Metal node distortion in tricoordinate Cu(I) accounts for the resultant unusual layer deformation, which was also investigated by theoretical and spectroscopy methods.

Needle-shaped colourless single crystals of **TEACu** were prepared by slow evaporation of a solution of $Cu(NO_3)_2{\cdot}3H_2O$, NaCN, and TEACl in 6 M NH_3aq. (Fig. S1, ESI†). **TEACu** crystallizes in the space group of *Ibam*. Anionic honeycomb-layers are composed of Cu^I ions bridged with cyanido ligands. These layers are flat within the *ab*-planes, but are constituted of highly distorted hexagonal units resulting in the distortion of the angles in the tri-coordinated geometry of the Cu^I centers (Fig. 2a and b). The angles of Cu–Cu–Cu of the hexagons are 102.7°, 109.5°, and 147.8° at 100 K. As a result, each hexagon unit exhibited a clear elongation along either the (110)- or the (1−10)-direction. This anisotropic distortion of the layers was induced by the presence of TEA cations in the interlayer spaces (Fig. 2c). Uniquely, two ethyl substituents of TEA fit diagonally into a hexagon, giving rise to the anisotropic distortion of the corresponding hexagon along the *a*-axis. The IR spectra of **TEACu** displayed a stretching peak of a cyanido group at 2117 cm^{-1} (Fig. S2, ESI†). TGA demonstrated that **TEACu** is stable up to 600 K (Fig. S3, ESI†).

We found that the flat layer of **TEACu** is extremely flexible, as confirmed by its TE behavior at 100–400 K. Variable temperature (VT)-single crystal X-ray diffraction results of **TEACu** provided the coefficient of TE (CTE) of $\alpha_a = -34.7(4)\ MK^{-1}$, $\alpha_b = 70.9(9)\ MK^{-1}$, $\alpha_c = 132(20)\ MK^{-1}$ ($M = 10^6$) (Fig. 2d and Table 1). These large CTE values are comparable with those of highly flexible undulating layered CPs.[33,34] Moreover, it is much more characteristic than anisotropic TE of other 2D-flat layered materials with rigid layers and same-signed in-plane TE (*i.e.* both axes in the plane show positive or negative TE behavior). The highly anisotropic in-plane TE behavior of **TEACu** is due to the structural transformation in which the stretched layer changes to its ideal geometry. Thus, the node distortion around the Cu^I centers is responsible for the transformation of the honeycomb layers. More specifically, the angles of Cu–Cu–Cu showed large changes to become closer to 120°, which is shown in a regular hexagonal lattice, as the temperature increased (Fig. 2e). The geometry-change of the hexagon in the layer is also shown by diagonal lengths between Cu ions of the

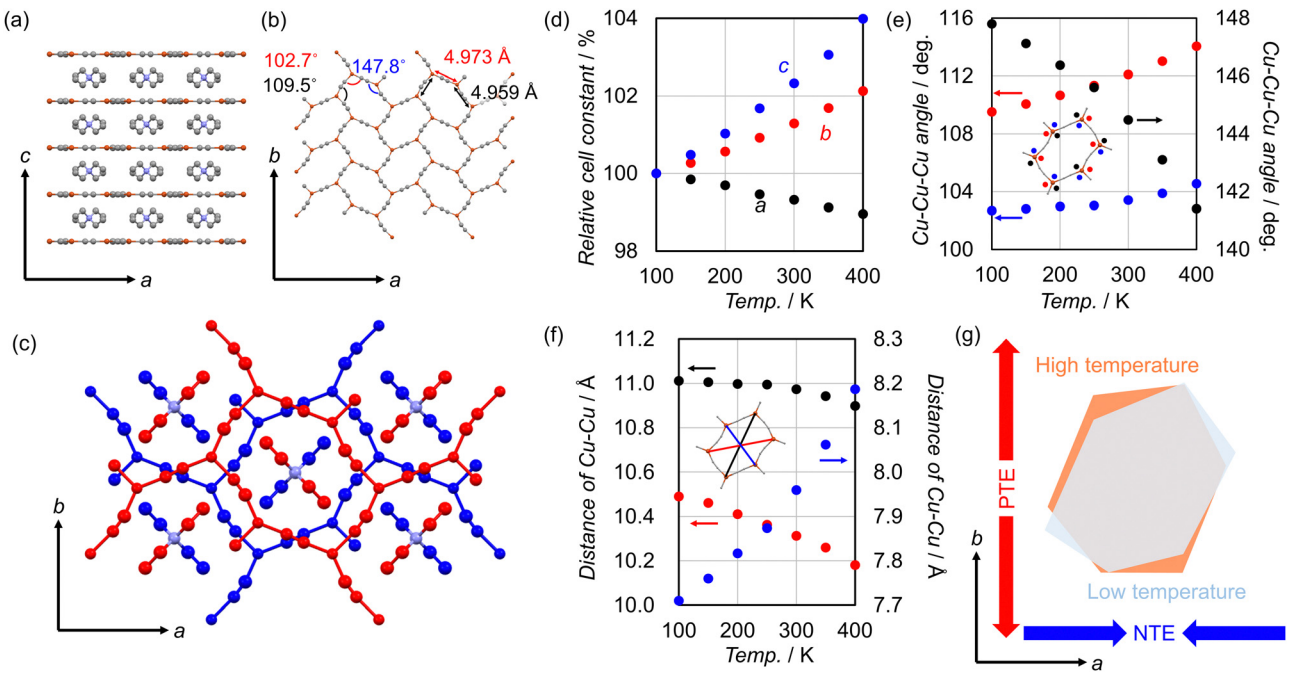

Fig. 2 Crystal structure of **TEACu** in the (a) stacking and (b) in-plane directions. Colour code: Orange; Cu, Light blue; N, Gray; C. Cyanido-bridges between Cu centers were disordered in the layer, and are presented as C atoms. (c) The packing structure of **TEACu** where red and blue coloured parts indicate upper and lower layers, respectively. (d) Relative cell length of **TEACu**. Black, red, and blue show the *a*-, *b*-, and *c*-axis, respectively. (e) Temperature variations of the angles of Cu–Cu–Cu and (f) the distances of the diagonal lines within a $Cu(CN)_6$ hexagon. (g) The schematic image of the deformation of a $Cu_6(CN)_6$ hexagon.

corresponding hexagon (Fig. 2f). These large decreases along the *a* axis and increases along the *b* axis are in accordance with the corresponding negative and positive TEs, respectively (Fig. 2g and Fig. S4, ESI†). Note that VT-IR and VT-Raman spectra displayed a noticeable shift for the stretching peaks of cyanido toward low energy regions (Fig. S5 and S6, ESI†). The luminescent properties of **TEACu** based on its copper-cyanido charge transfer were previously investigated at 77 K and room temperature, with an intensity maximum showing a slight shift from 380 to 371 nm.[32] These spectra changes reflected the local structural transformations involving the node distortion during the TE behavior.

The characteristic anisotropic deformation of flat layers involves the flexibility of tricoordinate Cu^{I} nodes, supported by quantum chemical calculation. The optimized structure of a local $[Cu(CN)_3]^{2-}$ part indicated C/N–Cu–C/N angles closer to 120° than **TEACu** (Fig. S7, ESI†). Therefore, it was demonstrated that a crystal packing effect on the coordination geometry of Cu nodes is present *via* the formation of the infinite honeycomb layers and corresponding anionic-layer stacking with cations. Uniquely, the HOMO of $[Cu(CN)_3]^{2-}$ is composed of the hybridization of the $3d_{x^2-y^2}$ and $4p_y$ orbitals (Cu) and σ_{CN} orbital (cyanido), suggesting that the overlap of these orbitals by decreasing the Cu node distortion results in the stabilization of the corresponding structure (Fig. S8 and S9, ESI†). Further calculation of a $[Cu(CN)_3]^{2-}$ moiety at 400 K demonstrated that its geometry changed to become close to an ideal Y-shape, which is less stable than that at 100 K by 0.31 eV. These results are in accordance with the flexible tricoordinate Cu^{I} node arising from the degree of freedom of the low-coordination on metal ions. Note that a similar role of flexible metal nodes on anisotropic TE has also been reported in other 3D metal-cyanidos,[35,36] metal-sulfocyanidos, and metal-selenocyanide compounds.[37]

Moreover, we found that all edge lengths between Cu ions of **TEACu** decreased as the temperature increases (Fig. 3, and Fig. S10, ESI†). Such counterintuitive shrinkage of the cyanido-bridge has been demonstrated by several cyanido-bridged negative thermal expansion materials such as Prussian Blue analogs.[38–40] Low energy transverse vibration of the cyanido was established to interpret unusual contraction of the cyanido-bridging between metal ions. In this sense, the vibrational calculations of the $[Cu(CN)_3]^{2-}$ moiety suggested that this part also exhibits similar vibration below 100 cm^{-1} (Table S2 and Fig. S11, ESI†). The single crystal X-ray analyses also corroborated that cyanidos exhibited large atomic displacement parameters in the vertical direction from the layers (Fig. S12 and S13, ESI†). Importantly, the resultant decreases of all edge lengths of the $Cu_6(CN)_6$ hexagon in **TEACu** are largely different from its analog of **PPh_4Cu** for which only two edges of the hexagon shrank while the other four expanded (Fig. 3).[30] Thus, these different TE behaviors of the anionic honeycomb layers demonstrate that cation species significantly influenced structural changes of the layers *via* intermolecular interaction. Comparing the closest distances between the cyanidos and hydrogens of the cations between **TEACu** and **PPh_4Cu**, **TEACu** exhibits weaker interaction than **PPh_4Cu**: the distances are 2.843 Å for **TEACu** and 2.779 Å for **PPh_4Cu** (both values are the shortest lengths at 250 K). These results indicate that the PPh_4 cations suppress the transverse vibration of four cyanidos within **PPh_4Cu**, and thereby intuitive expansion of the corresponding cyanidos occurs. A similar pinning effect for the transverse vibration on negative TE has been demonstrated by PBA *via* accommodation of lattice waters[41–43] and ScF_6 *via* Li^+ doping.[44]

In several 2D-materials, the unique properties of molecular species have been derived by sandwiching them between layers.[45–49] In this regard, we further analysed the conformation changes of TEA in the interlayer spaces of **TEACu**. Uniquely, TEA deformed to shrink within the layers along the large interlayer expansion (Fig. S14a and b, ESI†). This result indicates that the TEA appears to expand between layers at low temperatures. This cation deformation in **TEACu** follows the opposite trend to **PPh_4Cu** where PPh_4 expanded in the stacking direction *via* the coupling with the interlayer expansion (Fig. S14c, ESI†). These characteristic structural changes of spherical cations in the interlayer spaces demonstrate that the sandwiching system composed of $[Cu_2(CN)_3]^-$ also works as a platform bringing out the unprecedented molecular motion linked with the layer flexibilities.

In conclusion, we demonstrated the extreme flexibility of flat honeycomb layers of **TEACu** *via* its giant anisotropic in-plane thermal expansion. This unusual structural property was underpinned by distorted tricoordinate metal nodes. Thus, this work showed that even in conventionally rigid structural motifs, the material design incorporating node-distortion into the coordination network leads to the enhancement of structural flexibility and control of structural properties.

This work was supported by the Grant-in-Aid for Transformative Research Areas (A) "Supra-ceramics" (JSPS KAKENHI grant number JP22H05144 and JP22H05146). This work was also supported by the JSPS KAKENHI grant number

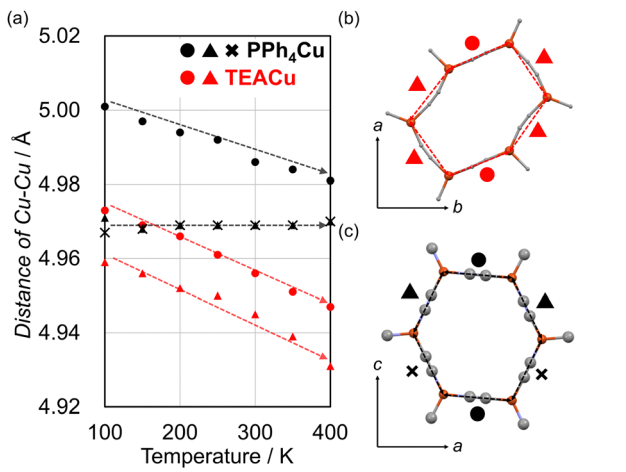

Fig. 3 (a) The distance of Cu–Cu in $Cu_6(CN)_6$ hexagons of **TEACu** (red) and **PPh_4Cu** (black). The hexagons of (b) **TEACu** and (c) **PPh_4Cu**. Circles, triangles, and crosses are consistent with the length shown in (a).

JP24K01457, JP21K18936, JP21H01905 and JP22K19052. This work was partially supported by the Cooperative Research Program of 'Network Joint Research Centre for Materials and Devices'. The computations in this work were performed using the computer facilities at the Research Institute for Information Technology, Kyushu University, at the Supercomputer Center, the Institute for Solid State Physics, the University of Tokyo, and at Cyberscience Center, Tohoku University.

Conflicts of interest

There are no conflicts to declare.

Notes and references

1 P. Kanoo, G. Mostafa, R. Matsuda, S. Kitagawa and T. K. Maji, *Chem. Commun.*, 2011, **47**, 8106–8108.
2 G. Y. Wang, L. L. Yang, Y. Li, H. Song, W. J. Ruan, Z. Chang and X. H. Bu, *Dalton Trans.*, 2013, **42**, 12865–12868.
3 A. a A. Massoud, M. A. M. Abu-Youssef, J. P. Vejpravová, V. Langer and L. Öhrström, *CrystEngComm*, 2009, **11**, 223–225.
4 X. Zhang, W. Zhang, R. Xiang, L. Lan, X. Dong, H. Sakiyama and M. Muddassir, *Polyhedron*, 2023, **244**, 116625.
5 Y. Jing, Y. Yoshida, T. Komatsu and H. Kitagawa, *Angew. Chem. Int. Ed.*, 2023, **62**, e202303778.
6 L. Lin, Q. Zhang, Y. Ni, L. Shang, X. Zhang, Z. Yan, Q. Zhao and J. Chen, *Chem*, 2022, **8**, 1822–1854.
7 J. Ogle, N. Lahiri, C. Jaye, C. J. Tassone, D. A. Fischer, J. Louie and L. Whittaker-Brooks, *Adv. Funct. Mater.*, 2020, **31**, 2006920.
8 J. Troyano, O. Castillo, J. I. Martínez, V. Fernández-Moreira, Y. Ballesteros, D. Maspoch, F. Zamora and S. Delgado, *Adv. Funct. Mater.*, 2017, **28**, 1704040.
9 J. Lu, Y. Yoshida, K. Kanamori and H. Kitagawa, *Angew. Chem., Int. Ed.*, 2023, **62**, e202306942.
10 Z. Zhang, Y. Nie, W. Hua, J. Xu, C. Ban, F. Xiu and J. Liu, *RSC Adv.*, 2020, **10**, 20900–20904.
11 B. K. Saha, S. A. Rather and A. Saha, *Eur. J. Inorg.*, 2017, 3390–3394.
12 P. Lama, A. Hazra and L. J. Barbour, *Chem. Commun.*, 2019, **55**, 12048–12051.
13 R. Ohtani, R. Yamamoto, H. Ohtsu, M. Kawano, J. Pirillo, Y. Hijikata, M. Sadakiyo, L. F. Lindoy and S. Hayami, *Dalton Trans.*, 2019, **48**, 7198–7202.
14 R. Ohtani, J. Yanagisawa, B. Le Ouay and M. Ohba, *ChemNanoMat*, 2021, **7**, 534–538.
15 A. S. Sergeenko, J. S. Ovens and D. B. Leznoff, *Chem. Commun.*, 2018, **54**, 1599–1602.
16 Y. Zhang, A. Sanson, Y. Song, L. Olivi, N. Shi, L. Wang and J. Chen, *Inorg. Chem. Front.*, 2022, **9**, 2036–2042.
17 S. J. Hibble, A. M. Chippindale, A. H. Pohl and A. C. Hannon, *Angew. Chem., Int. Ed.*, 2007, **46**, 7116–7118.
18 L. Zhao, J. Tang, M. Zhou and K. Shen, *New Carbon Mater.*, 2022, **37**, 544–555.
19 E. Kano, M. Malac and M. Hayashida, *Carbon*, 2020, **163**, 324–332.
20 M. J. McAllister, *Chem. Mater.*, 2007, **19**, 4396–4404.
21 D. Yoon, Y. W. Son and H. Cheong, *Nano Lett.*, 2011, **11**, 3227–3231.
22 Y. Ge, J. Li, Y. Meng and D. Xiao, *Nano Energy*, 2023, **109**, 108297.
23 Y. He, N. An, C. Meng, L. Xiao, Q. Wei, Y. Zhou, Y. Yang, Z. Li and Z. Hu, *ACS Appl. Mater. Interfaces*, 2022, **14**, 57328–57339.
24 Z. Wang and Y. Huang, *New J. Chem.*, 2023, **47**, 3668–3671.
25 C. Li, K. Wang, J. Li and Q. Zhang, *ACS Mater. Lett.*, 2020, **2**, 779–797.
26 K. Omoto, S. Aoyama, T. Galica, E. Nishibori, S. Katao, K. Yasuhara and G. Rapenne, *Dalton Trans.*, 2022, **51**, 17967–17972.
27 M. Pisacic, I. Kodrin, A. Trninic and M. Dakovic, *Chem. Mater.*, 2022, **34**, 2439–2448.
28 R. Ohtani, J. Yanagisawa, H. Matsunari, M. Ohba, L. F. Lindoy and S. Hayami, *Inorg. Chem.*, 2019, **58**, 12739–12747.
29 R. Ohtani, R. Yamamoto, T. Aoyama, A. Grosjean, M. Nakamura, J. K. Clegg and S. Hayami, *Inorg. Chem.*, 2018, **57**, 11588–11596.
30 Y. Iwai, M. Nakaya, H. Ohtsu, B. Le Ouay, R. Ohtani and M. Ohba, *CrystEngComm*, 2022, **24**, 5880–5884.
31 Y. Iwai, Y. Imamura, M. Nakaya, M. Inada, B. Le Ouay, M. Ohba and R. Ohtani, *Inorg. Chem.*, 2023, **62**, 18707–18713.
32 E. Colacio, *Inorg. Chem.*, 2002, **41**, 5141–5149.
33 S. A. Hodgson, J. Adamson, S. J. Hunt, M. J. Cliffe, A. B. Cairns, A. L. Thompson, M. G. Tucker, N. P. Funnell and A. L. Goodwin, *Chem. Commun.*, 2014, **50**, 5264–5266.
34 R. Ohtani, H. Yoshino, J. Yanagisawa, H. Ohtsu, D. Hashizume, Y. Hijikata, J. Pirillo, M. Sadakiyo, K. Kato, Y. Shudo, S. Hayami, B. Le Ouay and M. Ohba, *Chem. – Eur. J.*, 2021, **27**, 18135–18140.
35 C. S. Coates, J. W. Makepeace, A. G. Seel, M. Baise, B. Slater and A. L. Goodwin, *Dalton Trans.*, 2018, **47**, 7263–7271.
36 R. Ohtani, H. Matsunari, T. Yamamoto, K. Kimoto, M. Isobe, K. Fujii, M. Yashima, S. Fujii, A. Kuwabara, Y. Hijikata, S. I. Noro, M. Ohba, H. Kageyama and S. Hayami, *Angew. Chem., Int. Ed.*, 2020, **59**, 19254–19259.
37 R. Y. Williams-Sekiguchi, T. E. Karpiuk and D. B. Leznoff, *Can. J. Chem.*, 2024, **102**, 266–274.
38 N. Shi, Q. Gao, A. Sanson, Q. Li, L. Fan, Y. Ren, L. Olivi, J. Chen and X. Xing, *Dalton Trans.*, 2019, **48**, 3658–3663.
39 K. W. Chapman, P. J. Chupas and C. J. Kepert, *J. Am. Chem. Soc.*, 2006, **128**, 7009–7014.
40 Q. Gao, N. Shi, Q. Sun, A. Sanson, R. Milazzo, A. Carnera, H. Zhu, S. H. Lapidus, Y. Ren, Q. Huang, J. Chen and X. Xing, *Inorg. Chem.*, 2018, **57**, 10918–10924.
41 S. Adak, L. L. Daemen, M. Hartl, D. Williams, J. Summerhill and H. Nakotte, *J. Solid State Chem.*, 2011, **184**, 2854–2861.
42 Q. Gao, J. Chen, Q. Sun, D. Chang, Q. Huang, H. Wu, A. Sanson, R. Milazzo, H. Zhu, Q. Li, Z. Liu, J. Deng and X. Xing, *Angew. Chem., Int. Ed.*, 2017, **56**, 9023–9028.
43 A. L. Goodwin, K. W. Chapman and C. J. Kepert, *J. Am. Chem. Soc.*, 2005, **127**, 17980–19781.
44 J. Chen, Q. Gao, A. Sanson, X. Jiang, Q. Huang, A. Carnera, C. G. Rodriguez, L. Olivi, L. Wang, L. Hu, K. Lin, Y. Ren, Z. Lin, C. Wang, L. Gu, J. Deng, J. P. Attfield and X. Xing, *Nat. Commun.*, 2017, **8**, 14441.
45 Y. Shimizu, M. Maesato and G. Saito, *J. Phys. Soc. Jpn.*, 2011, **80**, 074702.
46 V. Smetana, S. P. Kelley, H. Pei, A.-V. Mudring and R. D. Rogers, *Cryst. Growth Des.*, 2021, **21**, 1727–1733.
47 Y. Sekimoto, R. Ohtani, M. Nakamura, M. Koinuma, L. F. Lindoy and S. Hayami, *Sci. Rep.*, 2017, **7**, 12159.
48 U. Geiser, H. H. Wang, K. D. Carlson, J. M. Williams, H. A. Charlier, Jr., J. E. Heindl, G. A. Yaconi, B. J. Love, M. W. Lathrop, J. E. Schirber, D. L. Overmyer, J. Ren and M. H. Whangbo, *Inorg. Chem.*, 1991, **30**, 2586–2588.
49 Y. Zhang, K. Ruan and J. Gu, *Small*, 2021, **17**, e2101951.